



Effect of deep cryogenic treatment on microstructure, mechanical properties and machining performances of coated carbide tool

Binxun Li^{1,2} · Song Zhang^{1,2} · Tao Zhang^{1,2} · Jing Zhang^{1,2}

Received: 28 August 2018 / Accepted: 6 December 2018 / Published online: 12 December 2018
© The Brazilian Society of Mechanical Sciences and Engineering 2018

Abstract

Deep cryogenic treatment (DCT) has been acknowledged as an approach to modify metallic materials properties to enhance their performance. The effects of deep cryogenic treatment parameters (cryogenic temperature, cooling rate, soaking time and tempering temperature) on microstructure, mechanical properties and machining performance of Ti (N, C)–Al₂O₃-coated cemented carbide insert have been comprehensively investigated in this paper. First, microstructure examination results show that a decarburization phase was detected and the WC particles were refined after deep cryogenic treatment. Secondly, the hardness of the WC–Co substrate and the wear resistance of the coatings after DCT were elevated. In addition, the transformation from α -Co to ϵ -Co was observed, which is highly dependent on cryogenic temperature and soaking time. Finally, dry milling experiments were carried out and the results indicated that the tool wear resistance was improved and the experimentally measured cutting forces had lower values using cryogenically treated insert, which can be attributed to the dissolution of Co into WC yielding microplastic deformation as well as the enhanced wear resistance. This research can provide guidance for optimizing DCT parameters of coated carbide insert to acquire desired mechanical properties and improve cutting performance.

Keywords Deep cryogenic treatment · Coated carbide insert · Microstructure changes · Microhardness · Dry milling · Tool wear

1 Introduction

Recently, to satisfy the strict requirement of high product output, low cost, environmental-friendly and extended tool life as well as excellent surface integrity in metal machining, new cutting tools, such as cemented carbides, ceramics, cubic boron nitride (CBN), have been widely used to machining hard-to-machine materials [1–3]. Due to the outstanding physical and mechanical properties of cemented carbide, which combines high strength, toughness and wear resistance, it has been indisputably employed to conduct

high-speed machining. However, during high-speed machining, especially for dry machining, one of the major problems encountered in cutting operation is the extremely high temperature at the tool–chip contact surfaces [4, 5]. The excessive increase in temperature at tool–chip contact surfaces is prone to cause tool failure ahead of time compared with conventional machining or that cutting fluids involved in cutting process [6, 7]. To overcome these drawbacks, coatings are introduced to the cemented carbide tools by means of physical vapor deposition (PVD) or chemical vapor deposition (CVD). The coatings are applied to reduce the friction between chip and tool and also serve as thermal barriers to alleviate the thermal loads on tool base material [8]. Nonetheless, the resultant physical and mechanical properties of the cutting tools are mainly determined by metallurgical characteristics.

Deep cryogenic treatment (DCT), as a nondestructive and efficient material modification technology, has been extensively used to modify microstructure [9], improve hardness [10], toughness [11] and wear resistance [12] as well as functional performance during serving [13]. In terms of DCT,

Technical Editor: Márcio Bacci da Silva, Ph.D.

✉ Song Zhang
zhangsong@sdu.edu.cn

¹ School of Mechanical Engineering, Shandong University, 17923 Jingshi Road, Jinan 250061, China

² Key Laboratory of High-efficiency and Clean Mechanical Manufacture (Shandong University), Ministry of Education, Jinan, China

it means place the target material into an environment for a period, where the temperature is far below the ambient temperature, generally about $-180\text{ }^{\circ}\text{C}$ [14–16]. Podgornik et al. [17] found that the variation in mechanical, tribological and load-carrying capacity of the tool steels after DCT was closely related to chemical compositions. Li et al. [18] investigated the effect of DCT on the mechanical properties of high-vanadium alloy steel. Experimental work reveals that a large amount of dispersed carbide precipitation appeared and secondary carbide increased. As pointed out by Bensely et al. [19], the carburized steel showed prominent wear resistance after DCT compared with shallow cryogenic treatment and conventional heat treatment. According to Li et al. [20], the microstructure changes of IN718 superalloy subjected to DCT were explored and the grains were refined apparently. In addition, numerous investigations concerning DCT on cutting tools are also reported. Yong and Ding [21] concluded that the hardness, compression strength, wear resistance and fatigue life of the YG8 exhibit higher values apart from bending strength and toughness after DCT. The residual stress and martensite phase transformation from $\alpha\text{-Co}$ (FCC) to $\epsilon\text{-Co}$ (HCP) are account for the change in mechanical properties. Vadivel and Rudramoorthy [22] compared the cutting performance of coated carbide inserts prior to and after DCT with respect to surface roughness, power consumption and flank wear. In contrast to using untreated cutting insert, work performed by Sreeramreddy et al. [23] observed the lower cutting forces and flank wear as well as superior surface finish with cryogenically treated cutting tools. It can be drawn up that most of the research in the past mainly focused on metallic materials and cemented carbides. However, scant research on the effect of DCT on coated carbide cutting tool has been done. Similarly, few studies on evaluating the machining performance of cutting insert after DCT in dry milling process have been reported formerly. Therefore, a comprehensive study of DCT on coated carbide insert as well as machining performances evaluation is urgent.

In this research, the effects of DCT parameters (cryogenic temperature, cooling rate, soaking time and tempering temperature) on microstructure, mechanical properties and cutting performance of WC–Co cemented carbide indexable inserts with coating Ti (N, C)– Al_2O_3 based on orthogonal experimental design were investigated. The objectives of this research are several folds: (1) A detailed study is performed to identify the microstructure evolution, phase transformation and microhardness variation; (2) scratch tests are carried out to examine

the coating wear resistance; and (3) dry milling experiments are conducted to evaluate the machining performances with respect to flank wear and cutting forces under same material removal rate.

2 Experimental works

The raw material employed in the experiments is chemical vapor deposition (CVD) Ti (N,C)– Al_2O_3 (thickness $\sim 5.0\text{ }\mu\text{m}$)-coated WC–Co cemented carbide indexable insert (type XOMX090308TR-M08 F40 M, Seco Company), which is widely used in hard machining operation. The physical properties of the tungsten carbide (WC–Co) insert are listed in Table 1. As given in Table 2, four DCT factors (cryogenic temperature, cooling rate, soaking time and tempering temperature) with five levels were adopted. Standard *L25* (54) orthogonal design experiments (Table 3) were conducted. Five levels of each factor were denoted as ‘–2,’ ‘–1,’ ‘0,’ ‘1’ or ‘2.’ The DCT experiments were performed in a Cryoprocessor (type SLX-30, Cryopower Company) controlled by a computer with liquid nitrogen as the coolant liquid. The schematic of DCT procedure is shown in Fig. 1.

Metallurgical characteristic observation including grain size evolution and phase transformation was performed by scanning electron microscope (SEM) and X-ray diffraction (XRD) technique, respectively. Image-Pro Plus software was applied to estimate the WC grain size diameter. Figure 2 shows the initial microstructure of WC–Co cemented carbide prior to DCT and average grain diameter as well as correspondent grain number. The average WC grain sizes were mainly in the range of $0.47\text{--}0.62\text{ }\mu\text{m}$. The higher appearance frequency is the WC grain with average size $0.62\text{ }\mu\text{m}$.

Mechanical properties including microhardness and coating wear resistance were measured, respectively.

Table 2 Factors and levels used in DCT experiments

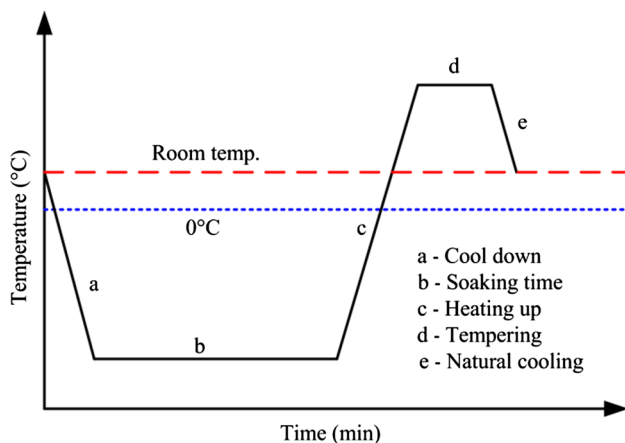
Factor	Level				
	–2	–1	0	1	2
A—cooling temperature ($^{\circ}\text{C}$)	–70	–100	–130	–160	–190
B—cooling rate ($^{\circ}\text{C}/\text{min}$)	2.0	3.5	5.0	6.5	8.0
C—soaking time (min)	60	90	120	150	180
D—tempering temperature ($^{\circ}\text{C}$)	20	60	100	140	180

Table 1 Physical properties of tungsten carbide (WC–Co) insert [24]

Material	Density (g/cm^3)	Elastic modulus (GPa)	Poisson's ratio	Specific heat ($\text{J}/\text{kg }^{\circ}\text{C}$)	Thermal conductivity ($\text{W}/\text{m K}$)	Thermal expansion ($\mu\text{m}/\text{m }^{\circ}\text{C}$)
WC–Co	14.5	696	0.25	260	28.4	5.2

Table 3 Design of experiment based on orthogonal method— $L_{25}(5^4)$

Experiment No.	Factor			
	A	B	C	D
1	-2	-2	-2	-2
2	-2	-1	-1	-1
3	-2	0	0	0
4	-2	1	1	1
5	-2	2	2	2
6	-1	-2	-1	0
7	-1	-1	0	1
8	-1	0	1	2
9	-1	1	2	-1
10	-1	2	-2	-2
11	0	-2	0	2
12	0	-1	1	-2
13	0	0	2	-1
14	0	1	-2	0
15	0	2	-1	1
16	1	-2	1	-1
17	1	-1	2	0
18	1	0	-2	1
19	1	1	-1	2
20	1	2	0	-2
21	2	-2	2	1
22	2	-1	-1	2
23	2	0	-2	-2
24	2	1	0	-1
25	2	2	1	0

**Fig. 1** Schematic of heat treatment procedure

Microhardness measurement was identified by means of a Vickers tester under constant load of 100 g with a dwell time 10 s. Scratch test with a load linearly increased from 0 to 100 N was applied to evaluate the coating wear resistance while sliding against diamond ball.

To appraise the machining performances of the deep cryogenically treated inserts, dry milling experiments of AISI H13 steel (50 ± 1 HRC) were carried out with the same material removal volume (5000 mm^3) on a CNC vertical machining center (ACE-V500, DAEWOO). The cutting speed was set as 200 m/min with constant feed rate 0.2 mm/tooth, and radial and axial depths of cut were 2.5 mm and 2.0 mm, respectively. Kistler piezoelectric dynamometer (type 9257B, Kistler-Morse Company) was used to gauge the cutting forces in three directions. Dino-Lite microscope was used for tool flank wear (VB) measurement. Here, flank wear was used as an indicator to characterize tool wear resistance.

3 Results and discussions

3.1 Microstructure evolution and EDS analysis

Figure 3 shows the SEM micrographs of the WC–Co cemented carbides after DCT. Compared with the original microstructure shown in Fig. 1, a new interphase can be observed with gray color as indicated by red arrows. In addition, with the decreases in cryogenic temperature, the frequency of the occurrence interphase seems to ascend within unite area. Although a new interphase was appeared after DCT, the morphology and distribution of WC particles show no pronounced distinction before and after DCT. In terms of new interphase, EDS was conducted to determine and compare the chemical composition of each phase. The chemical compositions of each phase are listed in Table 4 (Fig. 4). Figure 5 shows that the percentage of binder phase Co in the interphase is higher than that in WC phase, which means that DCT contributes to the shift of Co into WC phase. However, the ratio of carbon in the interphase is slightly decreased, which referred as decarburization phase. Thus, the DCT process promotes the precipitation of carbon from WC phase. The changes in WC particle sizes under different DCT conditions are shown in Fig. 6. Two exemplary cases, i.e., experiment No. 9 and experiment No. 25, were selected to demonstrate the variation in average WC grain size after DCT. The histograms describing frequency of WC grains with different sizes are presented in Fig. 6b and d. The sizes of vast majority of WC grains are between 0.42 and 0.57 μm for experiment No. 9 and between 0.35 and 0.49 μm for experiment No. 25. Apparently, the WC grain size variation trend shows a left shifting toward smaller grain size, as depicted by Gaussian curve in blue color. Assume that grain refinement of the WC–Co cemented carbide give rise to the enhancement of hardness.

Fig. 2 Metallurgical observation: **a** SEM image of initial microstructure; **b** histogram of grain diameters

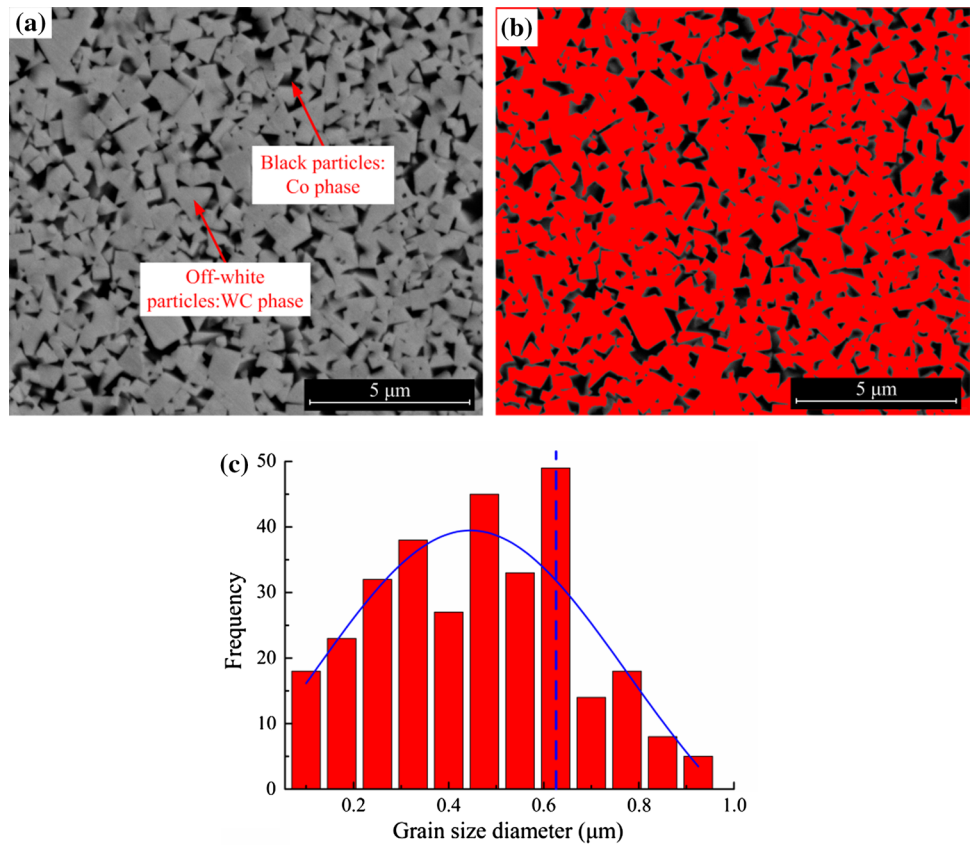


Fig. 3 SEM micrographs of deep cryogenically treated WC–Co cemented carbides: **a** experiment No. 1; **b** experiment No. 9; **c** experiment No. 20; **d** experiment No. 25

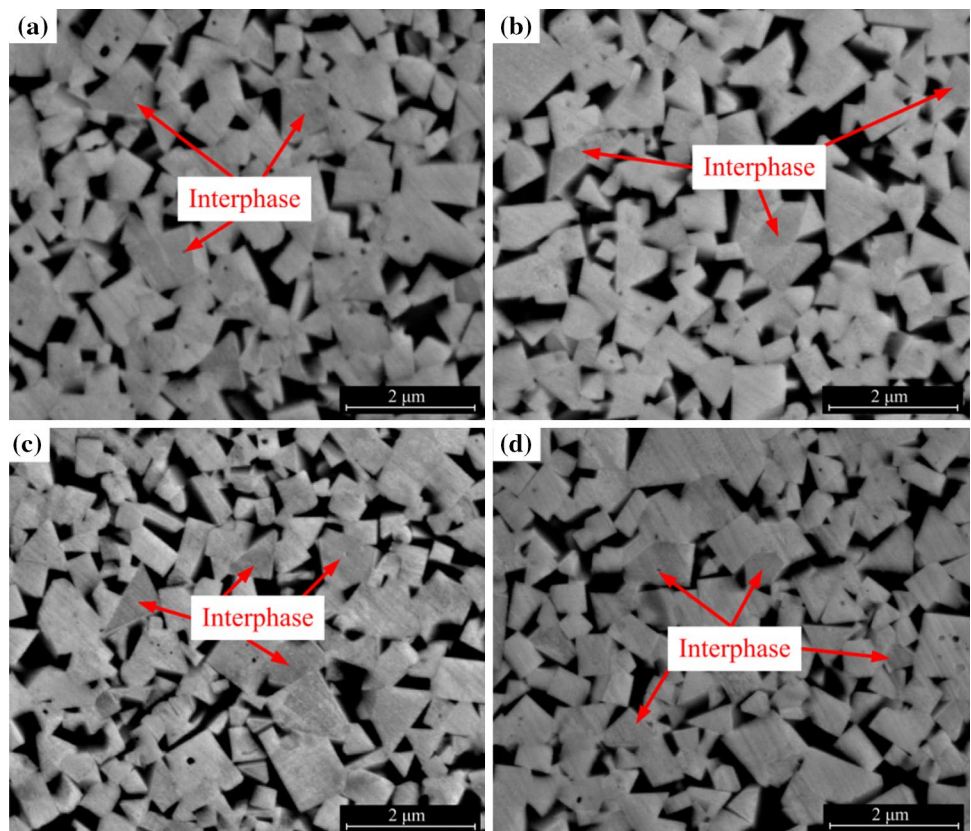
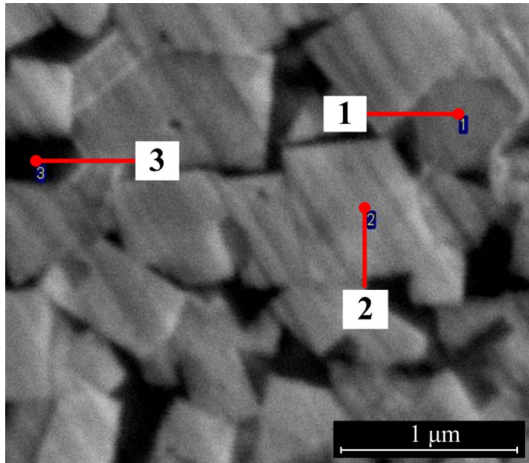
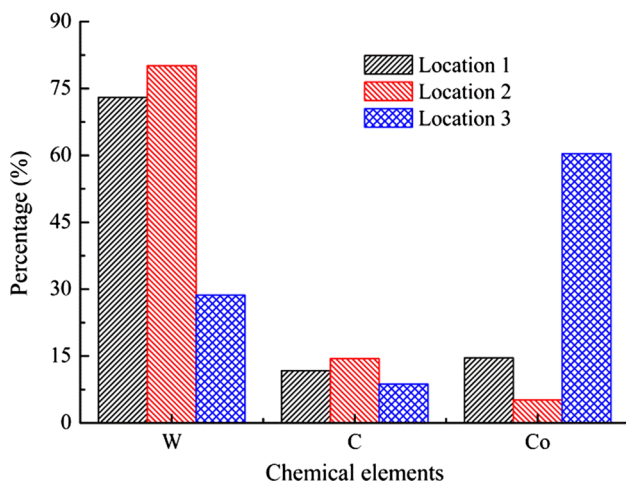


Table 4 Chemical compositions of different phase (wt%)

Location	Elements		
	W	C	Co
1	73.01	11.71	14.58
2	80.11	14.42	5.16
3	28.65	8.70	60.39

**Fig. 4** EDS analysis for different phase after DCT**Fig. 5** Chemical compositions of different locations

3.2 Phase transformations of Co phase

Figure 7 shows the XRD patterns of WC–Co cemented carbides before and after DCT. As far as the Co phase in cemented carbide is concerned, the α -Co phase with face-centered cubic structure and the ϵ -Co phase with hexagonal

close-packed structure can co-exist, as is also reflected by XRD spectrum. Based on the phase analysis, the integrated intensity of α -Co phase was reduced in various degrees under different DCT conditions. It is observed that the integrated intensity of α -Co corresponding to experiment No. 25 was the lowest. It can be inferred that a phase transformation from α -Co to ϵ -Co occurred after DCT. As the integrated intensity of the diffraction peak corresponding to ϵ -Co shows visually insignificant increase, a detailed estimation was performed as shown in Table 5. Apparently, the ratio of ϵ -Co was increased from 1.3 to 8.4%, while the ratio of α -Co was reduced from 29.0 to 21.3% in cryogenically treated insert compared with original cutting insert. Previous researches [25, 26] reported that the phase transformation from α -Co to ϵ -Co and the amount of ϵ -Co were highly dependent on cryogenic temperature and soaking time. It is believed that the phase transformation process can be confirmed and the amount of newly formed ϵ -Co was relatively little. Further, the ϵ -Co phase is harder to deform than α -Co phase owing to fewer slip systems, which is characterized by high hardness and lower friction coefficient [25].

3.3 Microhardness changes

Prior to DCT, the initial microhardness of the cemented carbide was measured approximately 1500 HV. Based on the orthogonal designed experiments, the appeared maximum microhardness 1827 HV was corresponding to experiment No. 20 with cryogenic temperature $-160\text{ }^{\circ}\text{C}$, cooling rate $8.0\text{ }^{\circ}\text{C}/\text{min}$, soaking time 120 min and tempering temperature $20\text{ }^{\circ}\text{C}$, while the minimum microhardness 1575 HV was corresponding to experiment No. 1 with cryogenic temperature $-70\text{ }^{\circ}\text{C}$, cooling rate $2.0\text{ }^{\circ}\text{C}/\text{min}$, soaking time 60 min and tempering temperature $20\text{ }^{\circ}\text{C}$. As to other sets of experiments, the microhardness was varied in the range of 1575 HV and 1827 HV. The microhardness values of the WC–Co cemented carbides show varying degrees of increment after DCT. Figure 8 shows that the cryogenic temperature and cooling rate have significant effect on microhardness compared with the effect of soaking time and tempering temperature. The microhardness increases with the elevated cryogenic temperature and cooling rate. Nonetheless, the microhardness values present inconspicuous variation when varying soaking time and tempering temperature, especially for tempering temperature. As reported in Ref. [26], ϵ -Co phase interior has fewer slip systems than that α -Co phase and impedes the generation of deformation, leading to a higher hardness. Therefore, WC grains refinement and the phase transformation from α -Co to ϵ -Co are responsible for the microhardness increase.

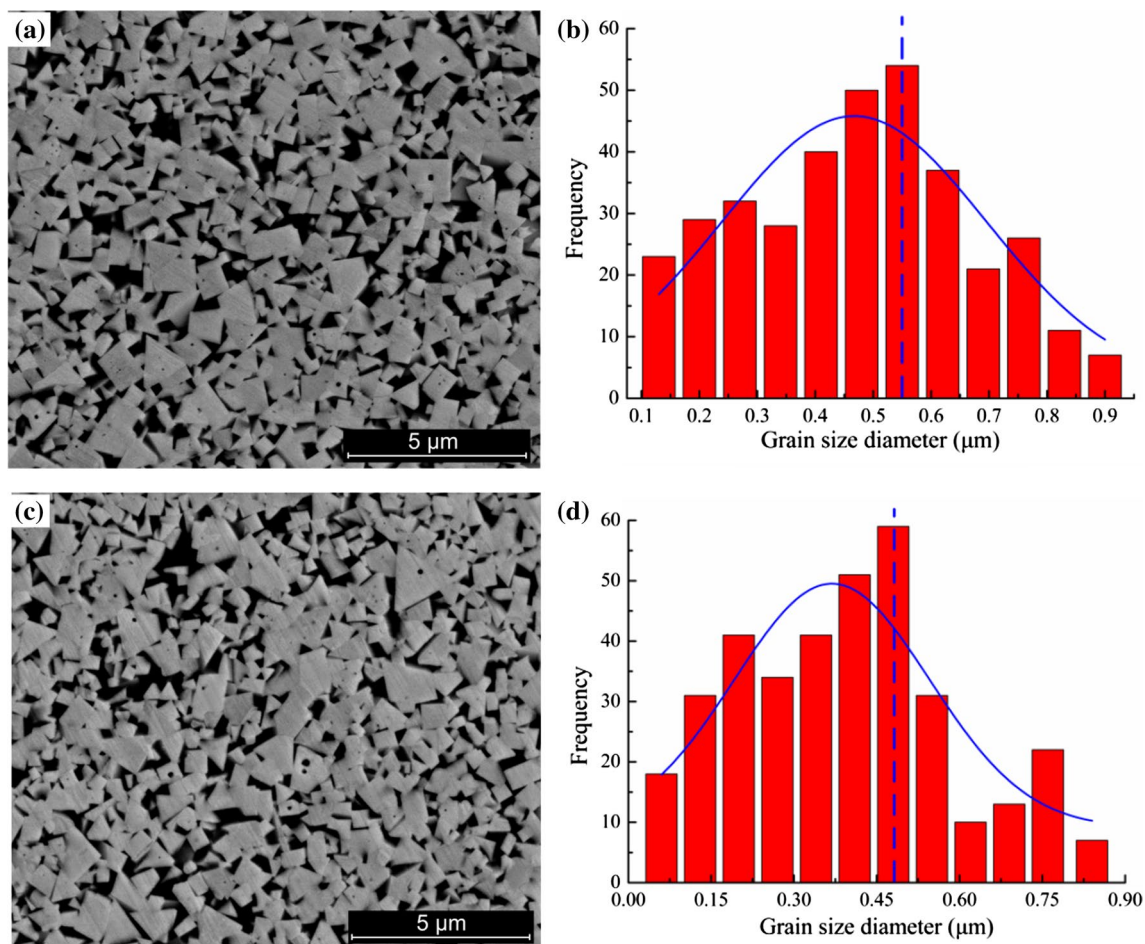


Fig. 6 Grain size variation with different DCT: a–b experiment No. 9; c–d experiment No. 25

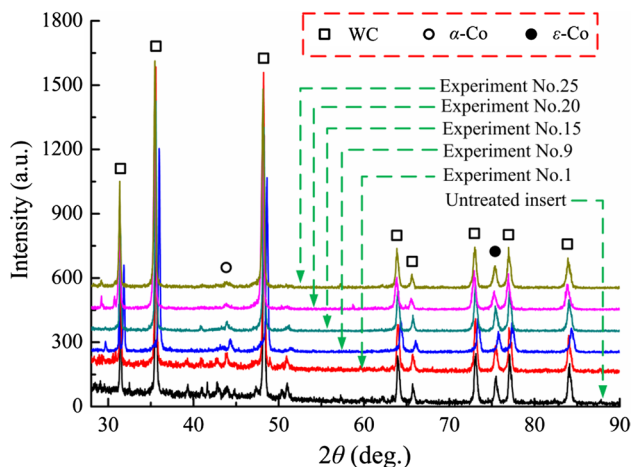


Fig. 7 XRD patterns of WC–Co cemented carbides before and after DCT

Table 5 Percentage variation of different phase before and after DCT (wt%)

Condition	Phase	Lattice constant	Percentage
Untreated	WC	2.9	67.2
	α -Co	3.5447	29.0
	ϵ -Co	3.42	1.3
	W, C, Co	7.826	2.5
Experiment No. 25	WC	2.9	62.8
	α -Co	3.5447	21.3
	ϵ -Co	3.42	8.4
	W, C, Co	7.826	7.5

3.4 Scratch test analysis

Figure 9 illustrates the SEM micrographs of worn coatings and element distributions of W after scratch tests. The regions with red arrows indicate the width of the scratch

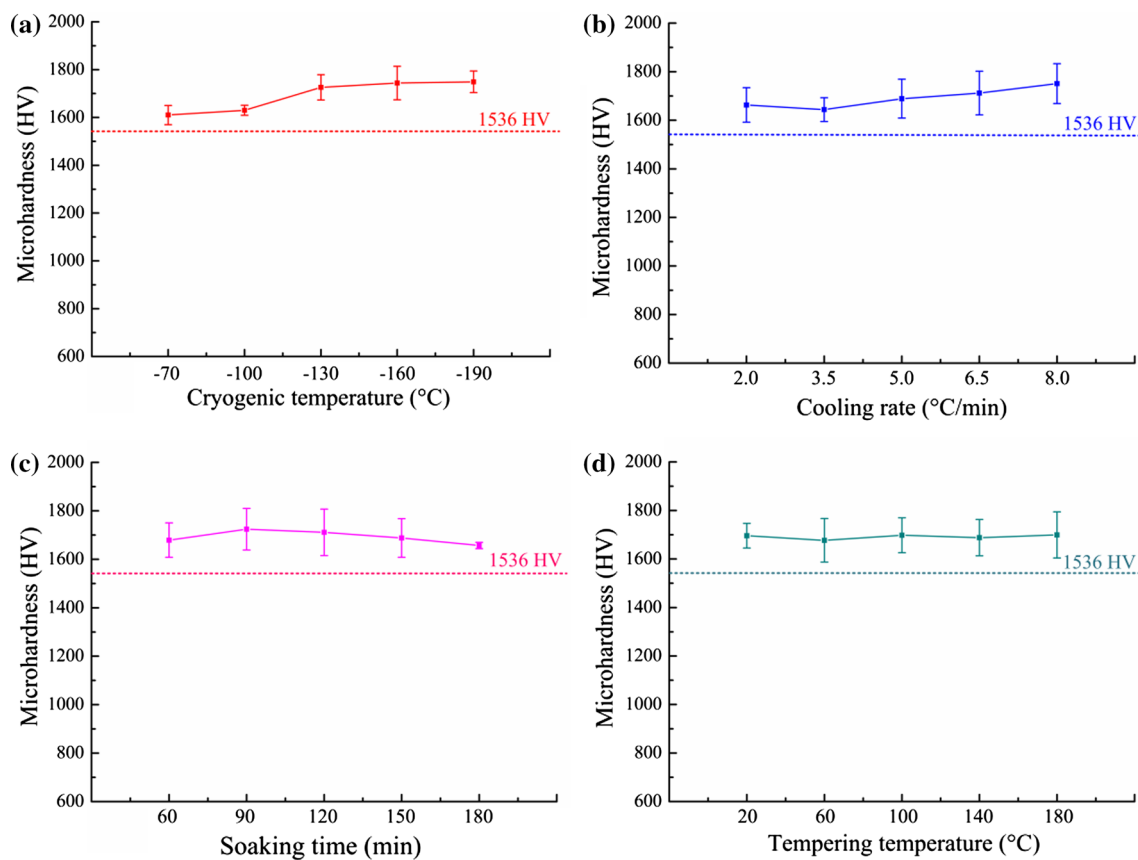


Fig. 8 Variation in microhardness: **a** cryogenic temperature; **b** cooling rate; **c** soaking time; **d** tempering temperature

at the end of the whole scratch length. Under the identical test conditions, the width of the scratch varies with different DCT conditions. The width of the scratches on tool coatings narrowed compared with untreated cutting insert, which proves the hardness improvement of the cryogenically treated cutting insert. From the right SEM images shown in Fig. 9, the distributions of element W on the worn coating surfaces before and after DCT demonstrate clearly distinction. For the untreated coated carbide insert, the exposure of element W in the substrate along the scratch states that the coating has nearly been damaged and flaked off. Regarding the cryogenically treated coated inserts, although the element W in substrate was still exposed on the worn surfaces, it is observed that the exposure area was quite limited, which is considered as a reflection of enhancement of coating wear resistance.

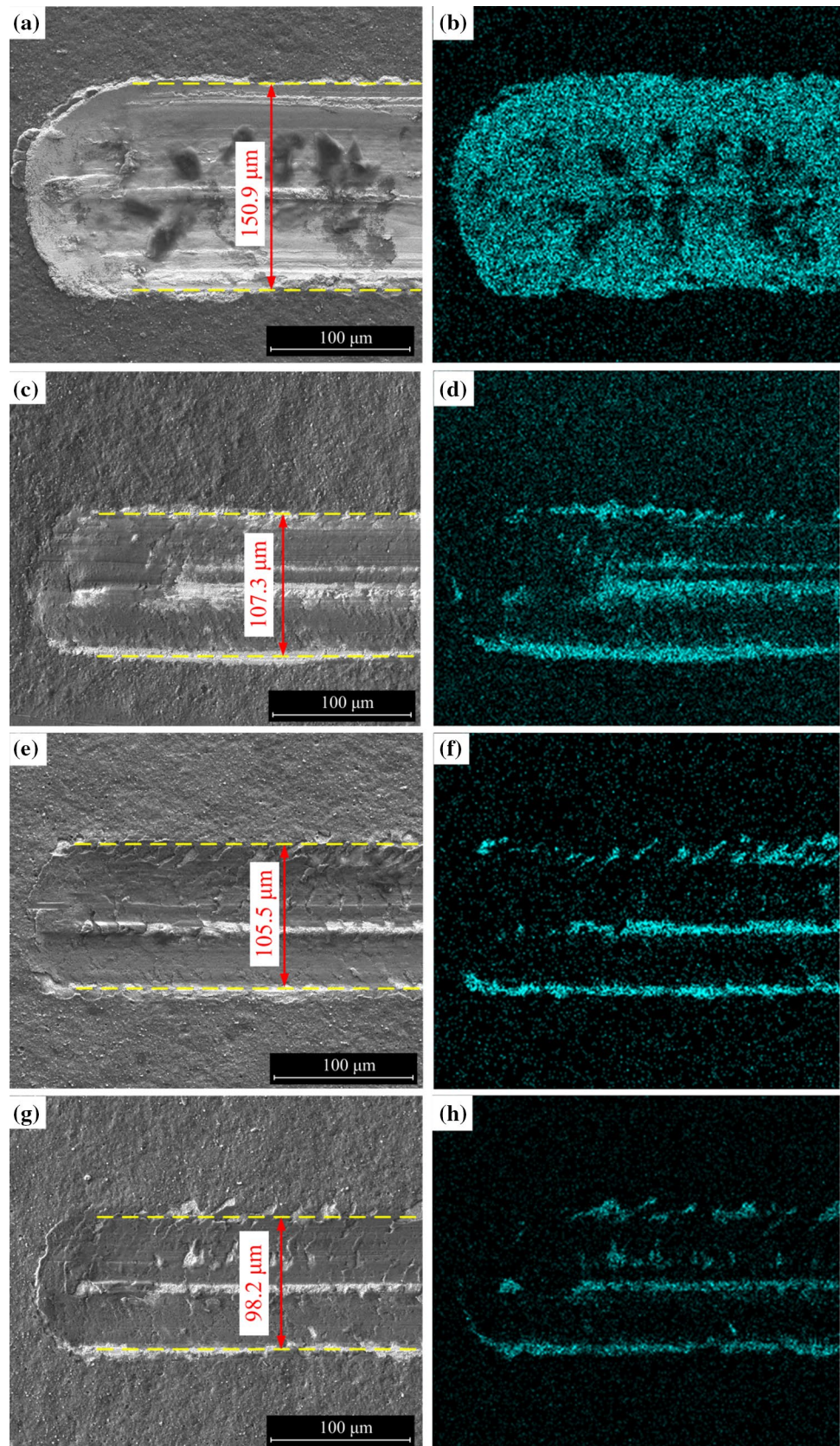
3.5 Cutting forces, tool wear and tool life

In this section, three exemplary Cases 9, 15 and 25 were selected to investigate the effect of DCT over cutting force

and tool wear. Figure 10 shows the comparison of cutting force in dry milling process using untreated and treated cutting inserts. In order to eliminate the statistic error due to tool wear, the cutting forces were measured and compared under the same material removal volume. Considering the close correlation of cutting forces and tool flank wear, the large cutting force is practically a reflection of severe flank wear. The experimental results indicated that the measured cutting force using treated milling insert was lower than that of using untreated ones. On the one hand, the friction between flank face and workpiece after coating flaking is reduced due to the good wettability of Co phase with WC phase. On the other hand, the precipitation of Co phase and dissolution into WC phase yield the possession of plastic deformation.

Figure 11 demonstrates the flank wear comparison between untreated and treated milling inserts after dry experiments. For untreated milling insert, the flank wear VB_{max} was supposed to reach 226.6 μm after completing the material removal volume 5000 mm^3 . In addition, the cemented carbide substrate as well as coating flaking

Fig. 9 SEM micrographs of worn surfaces (**a**, **c**, **e** and **g**) and element distribution of W (**b**, **d**, **f** and **h**): **a**, **b** untreated; **c**, **d** experiment No. 9; **e**, **f** experiment No. 20; **g**, **h** experiment No. 25



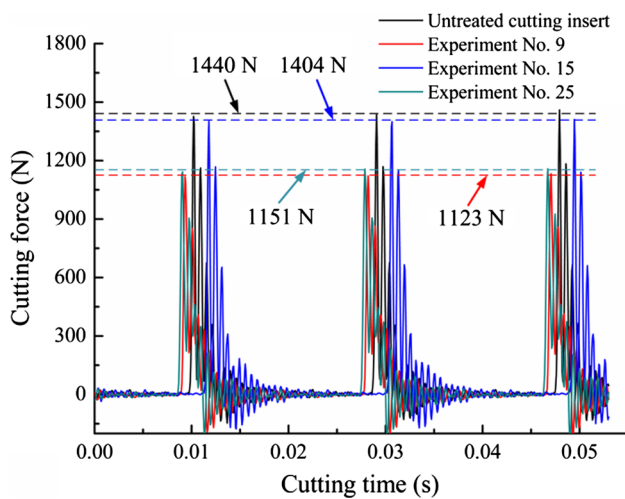


Fig. 10 Comparison of cutting forces in dry milling

was observed on tool flank face. On the contrary, the tool flank wears VB_{\max} of treated milling inserts were all lower than that of untreated ones. In Fig. 11c, the flank wear VB_{\max} was 167.9 μm , which is the most severe tool flank wear encountered in all dry milling experiments corresponding to experiment No. 15. Similarly, tool tipping was also occurred, which lead to the appearance of cemented carbide substrate and coating flaking. In terms of experiment No. 9, the cutting edge almost kept its original morphology except coating flaking on flank face, as illustrated in Fig. 11b. For the rest of milling tests, the tool flank wear VB_{\max} varies in the range of 52.1 μm and 226.6 μm . Thus, it can be concluded that the flank wear VB_{\max} of all treated milling inserts was reduced in comparison with untreated milling inserts. Therefore, the tool wear resistance in dry milling process was effectively improved after DCT. Moreover, the measured microhardnesses of cutting inserts corresponding to experiment Nos. 15 and 9 are, respectively, 1823 HV and 1624 HV. Reversely, higher hardness of the cutting insert corresponds to severer tool flank wear, while a low-hardness milling insert experiences relatively mild wear. Considering the intermittent character of milling operation, the cyclic severe shock is occurred when the cutting insert enters into the workpiece. Consequently, the brittle fracture of cutting edge is very likely to occur in dry milling process. Figure 12 depicts the variation

trend of flank wear with material removal rate (MRR). The MRR can be determined by using Eq. (1),

$$MRR = [\text{Initial weight} - \text{Final weight}] / [\rho \times \text{Time}] \text{ (mm}^3/\text{min)} \quad (1)$$

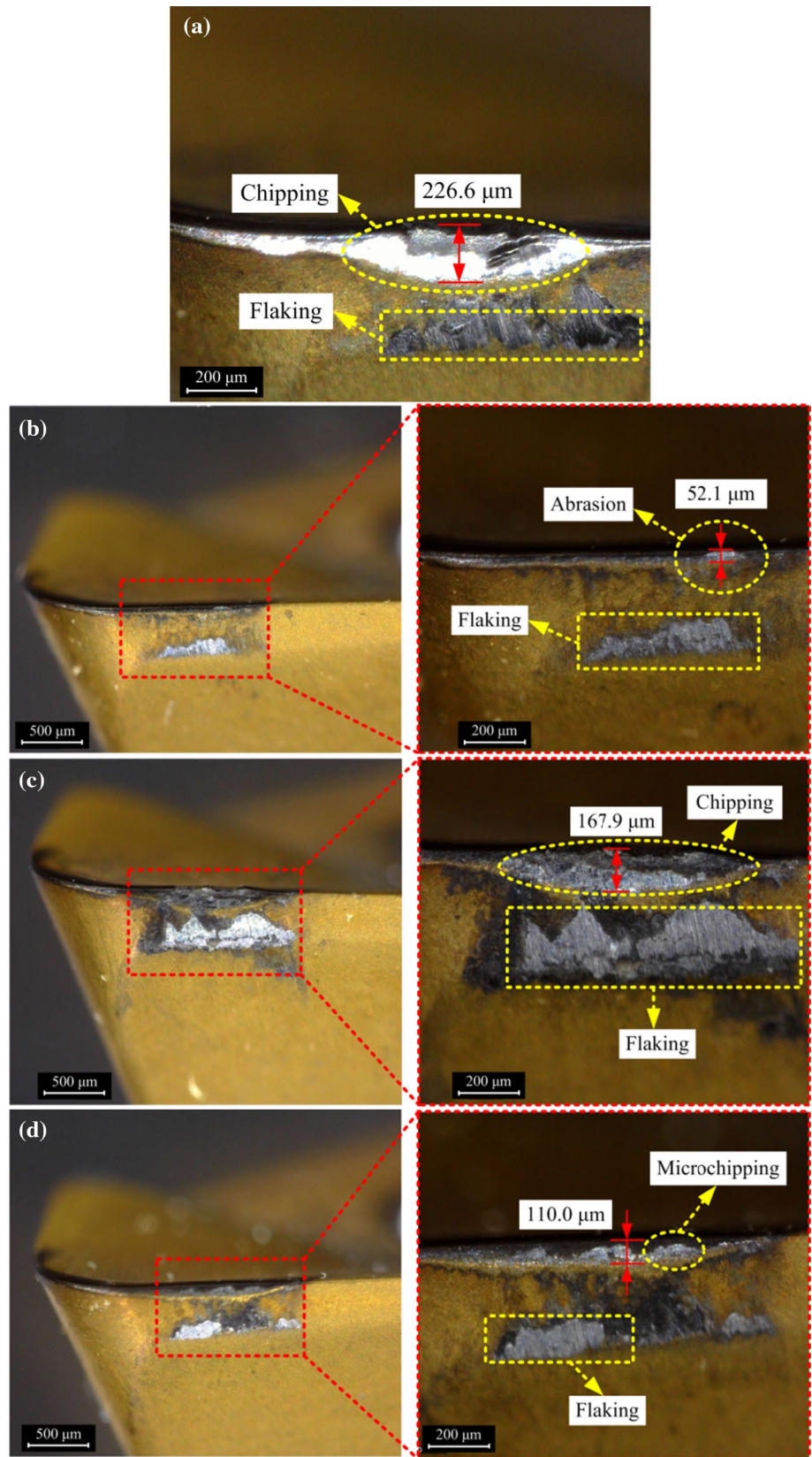
where ρ is the density of workpiece. Before the material removal volume reached 3500 mm^3 , the flank wear of treated and untreated cutting inserts was very close to each other. With the material removal volume increases, the flank wear of untreated cutting insert shows slightly higher than treated cutting insert. It is noted that a sharp rise of the flank wear with respect to untreated cutting insert was appeared when the material removal volume reached 9000 mm^3 . As shown in Fig. 12, the steep rise of too flank wear was the reflection of tool edge tipping. In contrast, severe cutting edge tipping was not noticed regarding cutting insert after DCT. As the binder phase, Co phase has the ability to bear plastic deformation to a certain degree during machining. Meanwhile, it has been confirmed that Co phase was precipitated out after DCT and dissolved into the hard and brittle WC particles. Taking these two factors into account, it is reasonable to believe that the wear resistance of the cutting tool was strengthened after DCT and the tool life was extended.

4 Conclusions

A design of experiment based on orthogonal method was performed to investigate the effect of deep cryogenic treatment on microstructure and mechanical properties of WC–Co cemented carbide insert with Ti (N, C)– Al_2O_3 coating materials and machining performances in dry milling. Based on the experimental results and analysis, the main conclusions are summarized as follows:

1. A new interphase named decarburization phase was formed and determined after DCT. The phase transformation from α -Co to ϵ -Co was also observed though little amount of α -Co phase was involved.
2. The hardness of WC–Co substrate and wear resistance of coating after DCT exhibited higher values than that of original insert. The improvement in the mechanical properties is mainly attributed to phase transformation and grain refinement.
3. In comparison with untreated coated carbide insert, deep cryogenically treated insert displayed higher wear resistance in dry milling operations.
4. The measured cutting force using deep cryogenically treated insert was slightly lower than that of untreated one.

Fig. 11 Flank wear after dry milling experiments with material removal volume 5000 mm³: **a** without DCT; **b** experiment No. 9; **c** experiment No. 15; **d** experiment No. 25



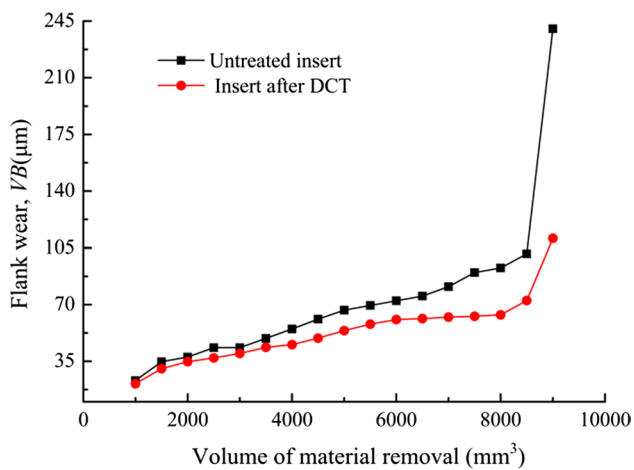


Fig. 12 Variation in flank wears with material removal volume

Acknowledgements This work was supported by the National Natural Science Foundation of China (Grants Nos. 51575321 and 51175309) and the Taishan Scholars Program of Shandong Province.

References

- Wang D, Xue C, Cao Y, Zhao J (2016) Fabrication and cutting performance of an $\text{Al}_2\text{O}_3/\text{TiC}/\text{TiN}$ ceramic cutting tool in turning of an ultra-high-strength steel. *Int J Adv Manuf Technol* 91(5–8):1967–1976
- Xu CH, Feng YM, Zhang RB, Zhao SK, Xiao X, Yu GT (2009) Wear behavior of $\text{Al}_2\text{O}_3/\text{Ti}(\text{C}, \text{N})/\text{SiC}$ new ceramic tool material when machining tool steel and cast iron. *J Mater Process Technol* 209:4633–4637
- Li A, Zhao J, Gong Z, Lin F (2016) Optimal selection of cutting tool materials based on multi-criteria decision-making methods in machining Al-Si piston alloy. *Int J Adv Manuf Technol* 86(1–4):1055–1062
- Novovic D, Dewes RC, Aspinwall DK, Voice W, Bowen P (2004) The effect of machined topography and integrity on fatigue life. *Int J Mach Tools Manuf* 44:125–134
- Zhang S, Guo YB (2009) An experimental and analytical analysis on chip morphology, phase transformation, oxidation, and their relationships in finish hard milling. *Int J Mach Tools Manuf* 49:805–813
- Xu CH, Feng YM, Zhang RB, Zhao SK, Xiao X, Yu GT (2009) Wear behavior of $\text{Al}_2\text{O}_3/\text{Ti}(\text{C}, \text{N})/\text{SiC}$ new ceramic tool material when machining tool steel and cast iron. *J Mater Process Technol* 209:4633–4637
- Grzesik W, Zalisz Z (2008) Wear phenomenon in the hard steel machining using ceramic tools. *Tribol Int* 41:802–812
- Goindi GS, Sarkar P (2017) Dry machining: a step towards sustainable machining—challenges and future directions. *J Clean Prod* 165:1557–1571
- Kumar S, Singh R, Batish A, Singh TP, Singh R (2016) Investigating surface properties of cryogenically treated titanium alloys in powder mixed electric discharge machining. *J Braz Soc Mech Sci Eng* 39(7):1–14
- Nanasa HG, Touazine H, Jahazi M (2016) Influence of cryogenic process parameters on microstructure and hardness evolution of AISI D2 tool steel. *Int J Adv Manuf Technol* 85(1–4):881–890
- Celik ON, Sert A, Gasan H, Ulutan M (2018) Effect of cryogenic treatment on the microstructure and the wear behavior of WC–Co end mills for machining of Ti6Al4 V titanium alloy. *Int J Adv Manuf Technol* 95(5–8):2989–2999
- Deshpande YV, Anghare AB, Padole PM (2018) Experimental results on the performance of cryogenic treatment of tool and minimum quantity lubrication for machinability improvement in the turning of Inconel 718. *J Braz Soc Mech Sci Eng* 40(1):1–21
- Paolo B (2009) Fatigue scatter reduction through deep cryogenic treatment on the 18NiCrMo5 carburized steel. *Mater Des* 30(9):3636–3642
- Liu Y, Shao S, Xu CS, Zeng XS, Yang XJ (2013) Effect of cryogenic treatment on the microstructure and mechanical properties of Mg–1.5 Zn–0.15 Gd magnesium alloy. *Mater Sci Eng A* 588(5):76–81
- Yong AYL, Seah KHW, Rahman M (2007) Performance of cryogenically treated tungsten carbide tools in milling operations. *Int J Adv Manuf Technol* 32(7–8):638–643
- Gill SS, Singh R, Singh H, Singh J (2009) Wear behaviour of cryogenically treated tungsten carbide inserts under dry and wet turning conditions. *Int J Mach Tools Manuf* 49(3):256–260
- Podgornik B, Paulin I, Zajec B, Jacobson S, Leskovišek V (2016) Deep cryogenic treatment of tool steels. *J Mater Process Technol* 229:398–406
- Li H, Tong W, Cui J, Zhang H, Chen L, Zuo L (2016) The influence of deep cryogenic treatment on the properties of high-vanadium alloy steel. *Mater Sci Eng A* 662:356–362
- Bensley A, Prabhakaran A, Mohan Lal D, Nagarajan G (2006) Enhancing the wear resistance of case carburized steel (En 353) by cryogenic treatment. *Cryogenics* 45:747–754
- Li J, Zhou J, Xu S, Sheng J, Huang S, Sun Y, Sun Q, Boateng EA (2017) Effects of cryogenic treatment on mechanical properties and micro-structures of In718 super-alloy. *Mater Sci Eng A* 707:612–619
- Yong J, Ding C (2011) Effect of cryogenic treatment on WC–Co cemented carbides. *Mater Sci Eng A* 528(3):1735–1739
- Vadivel K, Rudramoorthy R (2009) Performance analysis of cryogenically treated coated carbide inserts. *Int J Adv Manuf Technol* 42(3–4):222–232
- Sreeramareddy TV, Sornakumar T, Venkataramareddy M, Venkatram R, Senthilkumar A (2009) Turning studies of deep cryogenic treated p-40 tungsten carbide cutting tool inserts: technical communication. *Mach Sci Technol* 13(2):269–281
- Park S (2007) Development of a microstructure-level finite element model for the prediction of tool failure by chipping in tungsten carbide-cobalt systems. Ph.D. thesis, University of Illinois at Urbana-Champaign, Urbana, IL
- Wang G, Gu K, Huang Z, Ding P (2016) Improving the wear resistance of as-sprayed WC coating by deep cryogenic treatment. *Mater Lett* 185:363–365
- Zhang H, Chen L, Sun J, Wang W, Wang Q (2014) Influence of deep cryogenic treatment on microstructures and mechanical properties of an ultrafine-grained WC–12Co cemented carbide. *Acta Metall Sin* 27(5):894–900